

Fig. 11. Schematic of SWA-HIS with example particle trajectory. The cut-plane for the top part of the figure is that containing the Sun-spacecraft line and the direction of elevation deflection. The yellow shading represents the passage of direct solar light through the sensor and the red curve indicates a representative ion trajectory in this plane. The instrument has partial cylindrical symmetry extending from -33° to $+66^\circ$ out of the plane of the figure.

ions. The pixel resolution is $\sim 6^\circ \times 6^\circ$, which corresponds to a FoV comprising 16 azimuth and six polar sectors.

Figure 11 shows the two SWA-HIS ion optics subsystems: (1) The EA-IS is designed to achieve the required FoV and energy per charge (E/q) selection. An opening in the rear side of the EA-IS allows solar radiation to pass through unhindered. (2) The TOF telescope contains start and stop MCPs for time of flight measurement (τ) and SSDs for total ion energy (E_{Tot}) measurements. A carbon foil covers the optical path entrance to the TOF telescope as serves as a source of secondary electron to start the timing window.

Solar wind ions that enter the small aperture are steered by the IS into the EA. The EA voltage settings allow selection of ions within the appropriate E/q range to be transmitted into the TOF telescope. The IS plates, comprised of a deflector top plate (DFL Top), deflector bottom plate (DFL Bottom), and a “top-cap” serve plate to steer in ions over the range of $\pm 17^\circ$ in the polar direction. The EA-IS system is swept through voltages to scan the full elevation angle range and the full E/q range once per scan. Stray light and any ions outside this E/q range are suppressed by surface coatings and scalloping of the EA. The energy resolution of the EA is 6–10% and the elevation angle resolution is $< 3.5^\circ$ and have been verified by both ion optics simulations and laboratory calibration. The EA subsystem has a sufficiently large geometric factor ($\sim 2 \times 10^{-5} \text{ cm}^2 \text{ sr eV eV}^{-1}$ per 6° pixel) to measure 3D VDFs of Fe ions at 30 s time interval even during the lower flux and density slow solar wind conditions expected outside of 0.7 AU.

After passage through the SWA-HIS-EA and -IS subsystem, the ions converge at a focal plane that is co-aligned with the carbon foil. The entire TOF telescope, including the PA voltage gap, is designed to provide measurements ϕ , τ , E_{Tot} . The telescope has a simple interface to the SWA-HIS-EA subsystem via an aperture at ground potential. After passing through the

vacuum gap, which provides a stand-off distance sufficient for safe operation at the highest voltages, an accelerated ion penetrates a segmented ultra-thin ($\sim 0.9\text{--}1.1 \mu\text{g cm}^{-2}$) carbon foil and emits secondary electrons. These secondary electrons are deflected onto a Start MCP while maintaining their azimuthal location. The impact of secondary electrons on the Start MCP generates a start signal for TOF analysis. The ion continues through a nearly field-free volume before hitting the SSD array and emitting another set of secondary electrons that are deflected onto a Stop MCP. The electron impact generates a stop signal to complete the TOF (τ) measurement. A specially tailored electrode is situated between the start and stop MCPs to eliminate ion feedback between the two. The SSD array is comprised of 30 pixels spanning 96° in azimuth. Each pixel is comprised of a fully-depleted thin-window silicon detector with $500 \mu\text{m}$ depletion depth and $< 50 \text{ nm}$ dead-layer thickness. The pixel shape is a trapezoidal approximation to an arc segment, with an average width of 4.8 mm, a radial length of 3.7 mm, and an azimuthal width of 3° . The 96° azimuthal span will cover the required FoV and also accommodate azimuthal scattering from heavy ions as they pass through the carbon foil. The angle, TOF, and energy resolutions of the TOF-SSD subsystem are sufficient to meet all of the Solar Orbiter science objectives for SWA-HIS.

3.2.4. SWA-HIS design details

Figure 12 shows the SWA-HIS block diagram, indicating the functional grouping of the subsystems shown in Fig. 10. The figure includes all the PCBs contained in each subsystem, as described below.

HIS EA-IS subsystem. The EA-IS subsystem and supporting electronics were built by Institut de Recherche en Astrophysique et Planétologie (IRAP), in Toulouse, France. With the exception of the geometric factor, it is nearly the same design as the SWA-PAS electrostatic analyser. As SWA-PAS uses channeltron detectors, the SWA-HIS EA-IS geometric factor is $\sim 1/3$ smaller to accommodate the required MCP lifetime. The EA-IS system sits behind the carbon-carbon instrument heat shield and includes a rear exit for solar photon pass-through. The EA-IS is physically mounted to the outer housing of the SWA-HIS DS. The EA-IS body is grounded with a grounding strap to this same outer housing. Ions enter the instrument through a 3.5 mm slit in the SWA-HIS EA-IS; their elevation angle is controlled by top and bottom IS plates, with maximum voltages of $\pm 5.6 \text{ keV}$. The EA has a central radius of 70 mm with 2.3 mm hemisphere spacing and maximum voltage of $\pm 5.5 \text{ keV}$. The EA-IS entrance has knife edges to define the opening. The curved EA plates are scalloped and surface coated for light baffling. Electrical connections from the EA-IS run via cables down the outside of the TOF telescope and around the top of the ME box before mating up to the EA-IS HVPS inside the ME box. The EA-IS HVPS can be commanded into a sweeping mode where the voltages stored in the EA-IS table are stepped through with the timing specified in the table; static voltages were used during ground testing. Commanded parameters are monitored via flight software and the analogue readback of the direct voltage when sampled. The EA-IS stepping is fully synchronised with the TOF and energy data taken by the sensor via hardware handshakes across the optical link.

HIS detector section and readout electronics subsystem. The TOF telescope and associated electronics are isolated from the grounded housing that encloses them and separated from the housing by the PA gap. This gap is sized to keep electric

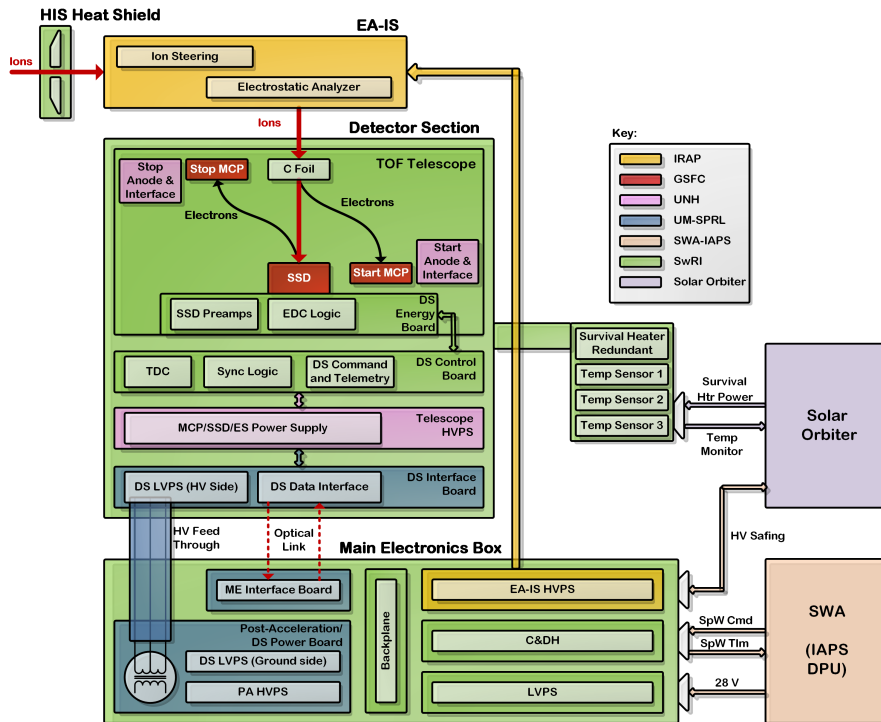


Fig. 12. HIS block diagram.

fields low according to Pachen's law in order to prevent voltage breakdown. The nominal -25 keV potential, supplied by the PA HVPS, is applied to the entire TOF telescope, accelerating ions entering from the EA-IS by 25 keV/e. The SWA-HIS TOF telescope and supporting electronics were built in the USA by a consortium comprising Southwest Research Institute (SwRI), University of Michigan (UMich), University of New Hampshire (UNH), and NASA GSFC. The interface between the EA-IS and DS subsystems is straightforward and controlled by an interface control document (ICD). This interface is an aperture at ground potential. The TOF telescope includes SSDs, MCPs, and associated electronics, control boards, and power supplies.

The ion entrance into the TOF telescope is fitted with a carbon foil and support grid. The ion path-length from the carbon foil to the SSD surface is 9 cm. The MCP Start and Stop stacks are made of two plates each in a classic chevron configuration with the front-side biased and the back side near-ground. The MCPs are mechanically clamped with tension springs and electrode contacts within the stack. Voltages are optimised for MCP throughput and vary with age, but are nominally set to 2.1 keV across the plate stacks. MCP gain is adjustable by increasing or decreasing the MCP bias voltage as needed and is anticipated to change over the mission lifetime. Azimuthal position can be obtained from the start position anode. The angular resolution is determined by the delay line with 2° strips. The TOF resolution, derived from the MCP signals, is <1.7 ns, with a TOF bin size of 0.64 ns. The TOF resolution is species and energy dependent and has been calibrated in the laboratory. Cross talk between Start and Stop MCP is virtually eliminated by a set of dedicated electrodes. The detector section's TOF and position measurements design was optimised with 3-dimensional electrostatic simulations (using SIMION¹) and hundreds of hours of ion testing on the detector section prototype. Additionally, ion feedback at both the Start and Stop MCPs is minimised by ensuring the bias angle on the exit plate is at least 15° to the normal of the anode and

applying only 50 V between the exit of the plate and the anode itself. Each SSD comprises one pixel, with 30 pixels mounted on ceramic carries spanning the azimuthal FoV. Angular resolution of 5° is limited by the size of the pixels and the required electronics for each pixel.

The isolated TOF electronics are floated at the same potential as the TOF telescope. These DS electronics include the detector section interface board (DSIB), the MCP HVPS, the DS control board (DSCB), and the DS energy board (DSEB). The DSIB supplies the low voltages for the DS (derived from the AC voltage riding on the PA-HVPS signal) and the DS side of the optical data communications link to the ME box. The MCP HVPS provides float and bias voltages for both the start and stop MCPs as well as the SSD bias voltage. All outputs are programmable. The DSCB uses an FPGA to perform the TOF measurement, time-to-digital conversion (TDC), application of commandable event logic, and combination of these signals with the energy measurement to form a partial PHA event word. DSCB event logic can be configured to trigger on events that have measurements of SSD energy only, TOF only, or both. The DSCB then sends events to the DSIB for transmission to the ME through the optical data communications link and provides fault detection, isolation and recovery (FDIR) capabilities. The DSEB houses the SSDs and collects and processes signals from the SSDs, using a specially designed, 32 channel ASIC. The DS also holds the HV side of an LVPS for powering these DS electronics. Measurement data are transmitted to the ME at ground potential via an optical link on the DSIB. The bulk of this data are PHA event words, containing the measurements of TOF (9 bits), total energy (9 bits), azimuthal angle (6 bits), SSD ID (5 bits), decimation class (3 bits) and multi-SSD flag (1 bit). These bits are streamed across the optical link and paired with the rest of their measurement information (e.g. E/q step, elevation angle) in the ME.

HIS main electronics. The ME sit below the TOF system at spacecraft potential. The ME includes: the LVPS, the Command and Data Handling Board (C&DH), the EA-IS HVPS, the optical link, and the PA-HVPS. The LVPS supplies all of the low

¹ <https://simion.com/docs/simion8brochure.pdf>

voltages to the other ME boards, as well as a 20 V_{pp} (peak-to-peak) square wave AC supply to link low voltages to the detector section. The C&DH board controls the balance of the instrument and houses the memory, processor and flight software, as well as FDIR functions. The EA-IS HVPS, built by IRAP, drives the EA-IS voltages. This HVPS consists of a pair of commandable bulk-supplies and commandable outputs for each of the electrodes in the EA-IS system. The optical link provides the ME side of the system for digital communication to the DS. The PA-HVPS provides the floating voltage to the detector section as well as a pathway for low voltages to cross the post-acceleration gap. The PA-HVPS provides DC-to-DC power conversion to lift the DS to -25 keV referenced to the ME ground potential. It also provides AC-to-DC conversion between the LVPS and the DS electronics. DC power is passed from the PA-HVPS across the PA gap into the detector section through a high voltage feed-through that provides both electrical isolation from ground potential and thermal isolation from the detector section. Heat generated by the AC-to-DC converter is coupled to the ME box chassis ground through a thermally conductive HV insulator.

The LVPS is free-running upon application of power with AC-link voltage commandable to on or off. Both HVPS supplies have enables and commanded output voltages. Electrical interface to the spacecraft is via a 28 V regulated, switched power line as well as a SpW data interface through the DPU. The DPU interface is limited to a SpW data link and the digital data that cross that link (i.e. heartbeats and FDIR information in addition to the normal HK and science data). The ME passes the event word to the C&DH, where the SWA-HIS flight software (FSW) completes it with the addition of the E/q (7 bits) and elevation step (4 bits) information. Each PHA word is a total of 46 bits. The C&DH board includes a SPARC-8 micro-controller (32-bit data bus) with 128 KB of external programmable read only memory (PROM), 2 MB of magnetic random access memory (MRAM) and 16 MB of static random access memory (SRAM). The ME also include temperature sensors and survival heaters. Radiation shielding in the ME is provided by the aluminium enclosure.

The SWA-HIS FSW controls the instrument primarily through the science programme, which is separated into several tasks. The “main” task runs at 10 Hz and performs processes such as receiving and validating commands, building and sending HK-related telemetry packets, running macros, sweeping EA-IS HV, and monitoring safety limits. The “science” task handles the fairly complex processing required to meet SWA-HIS science requirements, such as collecting PHA words and sorting them into bins subdivided by priority, counting them into priority rate and on-board VDF histograms, and randomly selecting them for inclusion in telemetry. SWA-HIS was designed to handle events at rates of up to 100 kHz, including both the hardware and software aspects of the PHA processing pipeline. Many features are table-based to allow for easier reconfiguration, including many EA-IS parameters (e.g. voltage steps, dwell & settling times), PHA handling parameters (e.g. E-TOF boxes for each priority range and E/q , sizes of buffers and number of PHA words per energy scan), and data product specifics (e.g. sizes and ions chosen for on-board VDFs). It also handles data compression, memory operations and scrubbing.

3.2.5. SWA-HIS testing, characterisation and calibration

SWA-HIS has been characterised at both subsystem and instrument levels, with subsystem testing taking place at UMich, SwRI, UNH, GFSC, and IRAP. SWA-HIS has been calibrated at the instrument level at three different facilities, during four test sessions, as summarised in Table 2.

Table 2. SWA-HIS ground calibration programme.

	Location	Dates	Configuration	Scope of calibration
1	H30 at SwRI	Sep–Oct 2015 and Jan–Mar 2016	EA-IS	Optimisation of the EA-IS voltages
2	H19 at SwRI	Sep–Nov 2016	Complete sensor minus EA-IS	Mass (1–56) and energy (0.1–450 keV) response
3	Mefisto at Bern	Jan–Feb 2017	Complete sensor	Charge (1–4), mass (1–84) and energy/charge (3–60 keV/e) response
4	H19 at SwRI	Mar–Apr 2017	Complete sensor	Geometric factor

Test session 1 involved testing the EA-IS subsystem at SwRI. Testing lasted 36 days where the EA-IS was combined with a mock-up TOF section with a phosphorus screen in the SSD plane. Particle interactions with the phosphorus screen were imaged with a camera. This setup did not allow for TOF measurement, but was dedicated to evaluating the electro-optics and ion trajectories, with full post-acceleration. The ion beam consisted of Ar⁺ with energies ranging from 1 keV to 40 keV. Illumination of the EA-IS aperture was completed with a broad, uniform, parallel beam larger than EA-IS aperture. During this test, the EA-IS and mock-up TOF were powered by laboratory equipment.

Calibration of the EA-IS addressed a number of aspects of performance. These included determination of: Energy-angle response of EAIS; optimal tuning of the EAIS voltages; elevation and azimuth response; energy-per-charge resolution; elevation angle resolution; ion optics and ion focus onto SSD; and relative efficiency.

Test session 2 was completed at SwRI with only the TOF telescope and associated electronics. It consisted of 5 days of beam testing without post-acceleration and 4 days of testing with full post-acceleration of the ion beam. The TOF telescope was subjected to a beam of H⁺, H₂⁺, He⁺, N⁺, H₂O⁺, Ne⁺, Mg⁺, N₂⁺, Ar⁺, Ar²⁺, Ar³⁺, and Fe⁺. Beam energies ranged from 0.3 keV to 450 keV (1.35 MeV for Ar³⁺), with beam intensities in the kHz range. The ion beam was vignettted by a 3 mm dia hole (7 mm²) to simulated a pencil beam incident on the TOF aperture. Flat ion beam illumination of the TOF aperture was also conducted. During 80 h of operations there were no spurious events detected.

Test session 3 was completed in the Mefisto vacuum chamber at the University of Bern with the full integrated sensor. Testing lasted 21 days and was conducted with all voltages operating at nominal flight-like settings. The instrument was subjected to a beam of H, H₂, He, C, N, O, F, S, Ar, Ca. Beam energies ranged from 3 keV to 60 keV, with beam intensities in the kHz range. A vignettted beam through a 2 mm diameter hole illuminated the instrument aperture. The testing included over 200 h of operations with no spurious events record.

Test session 4 was conducted at SwRI and included 5 days of testing of the integrated instrument with full PA voltages applied. The instrument was subjected to a beam of H, He, and N. Beam energies ranged from 0.3 keV to 60 keV, with beam intensities in the kHz range. The instrument aperture was illuminated with a flat beam. In over 80 h of operations no spurious events were recorded.

Overall, during test sessions 2–4, a number of aspects of sensor performance were assessed. These included the following: aliveness of the sensor; communication at various speeds;

Table 3. Species and charge states used during calibration.

HIS elements and charge states						
	1	2	3	4	5	6
H	Yes					
He	Yes					
C	Yes	Yes	Yes	Yes		
N	Yes	Yes	Yes			
O	Yes	Yes	Yes			
F	Yes	Yes				
Ne	Yes	Yes	Yes	Yes		
S	Yes	Yes	Yes	Yes		
Ar	Yes	Yes	Yes	Yes	Yes	Yes
Fe	Yes	Yes				
Kr	Yes	Yes	Yes	Yes		

Notes. “Yes” indicates the ion species was generated and measured, blank cells indicate the ion species was not able to be generated in the lab, and greyed out cells indicate the ion does not exist in nature.

coincidence logic; energy, elevation, and azimuth acceptance and resolution; TOF and energy resolution for various species; TOF and energy range; constant fraction discrimination thresholds on detectors; operation at high fluxes; and proton and alpha rejection capability. Table 3 shows the elements and the charge states collected during ground calibration.

Figure 13 shows the dependency of collected TOF bin and collected energy bin as functions of beam energy. Data collected using the Bern facility and the SwRI accelerator agree very well to each other and can be well approximated by a forward model that takes into account losses through the foil, and the dependency of detected energy to particle mass and energy.

HIS in-flight calibration. HIS will be calibrated in-flight to check the instrument performance parameters established during ground calibrations. Internal calibration of the SWA-HIS sensor will include validating instrument efficiencies and comparing the instrument response to various ions. Start, Stop, and SSD rates will independently measure instrument efficiencies, which will be monitored as a function of time, as detector responses may decline with age. In particular, the SSD may experience an increase in dead layer or reduced signal amplification over time, and MCP performance may degrade due to large cumulative radiation events. The MCP gain will be monitored and bias voltages increased to compensate for losses in gain. The measurements will be compared with our forward model for ion identification and adjustments made as necessary. Internal calibration capabilities include time and energy test pulse generators. Further calibration includes a test of the cross suite data link as well as cross-calibrations with SWA-PAS. Such internal test and suite-level cross calibrations will be performed routinely at UMich. Gain measurements for SSD and MCPs will be made every six months and after major SEP events, potential temperature increases near perihelion, or other spacecraft occurrences that could affect efficiencies. MCP and SSD voltage adjustments will be made as appropriate.

3.2.6. Summary of SWA-HIS specifications at delivery

The SWA-HIS calibration campaign had two major goals. Firstly, to establish all needed parameters to be able to invert the measurements to be collected in flight into physical units.

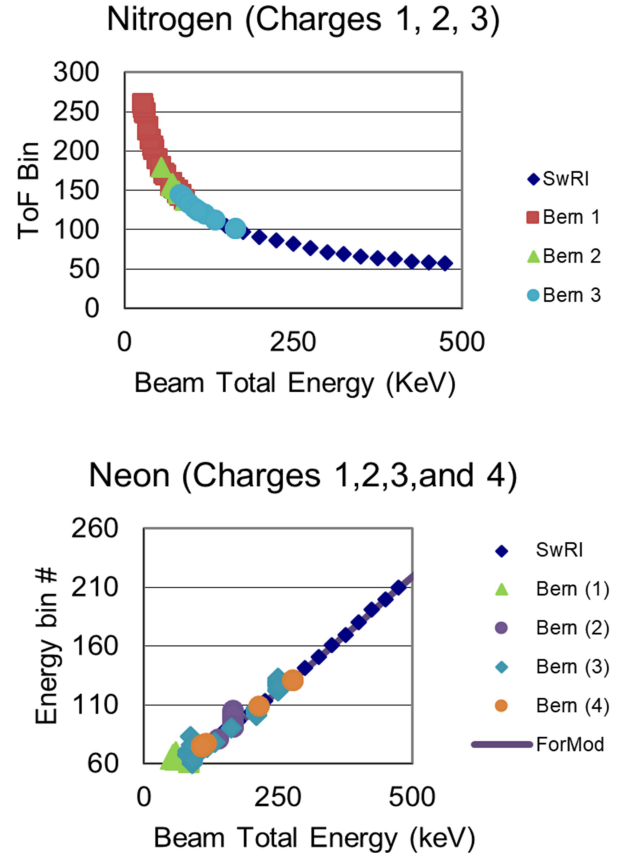


Fig. 13. Time-of-flight (*top*) and energy (*bottom*) response to beams of N and Ne as function of beam energy.

Secondly, to prove that the instrument has performance that will fulfil all Level-1 requirements.

Table 4 summarises the most important characteristics of the SWA-HIS sensor; rows colour-coded in blue show the project-defined Level-1 requirements. All properties of the SWA-HIS sensor are as expected from the design, and are compatible (and indeed most of the time better) with those needed to fulfil the Level-1 requirements. Some of the parameters reported in Table 4 are for an average configuration of the sensor: specifically, while the normal E/q resolution is $\sim 8\%$ and the geometric factor per pixel is $\sim 1 \times 10^{-5} \text{ (cm}^2 \text{ sr eV eV}^{-1}\text{)}$, by tuning the EA and IS voltages it is possible to increase the E/q resolution while lowering the GF, and vice versa. In-flight performance will be used to establish the most appropriate compromise between these two values.

It must be noted that for large azimuthal angles (ϕ) and for elevation angles (θ) out of the nominal orbit plane of the spacecraft ($\theta > 7^\circ$, $\theta < -7^\circ$), the centres of the elevation look-directions change slightly from the nominal. This property was expected for both SWA-HIS and SWA-PAS, and has been factored into the calibration files, such as to enable proper reconstruction of the VDFs.

The mass separation capabilities of SWA-HIS are illustrated in Fig. 14, which shows an energy versus TOF spectrogram obtained during laboratory testing. The track of Ar (doubly ionised in this series) is well separated from the track of Ne for all energies down to 100 keV. This energy corresponds to a charge state of 4, smaller than that expected for Ne in the solar wind. For higher charge state, the energy after PA will be larger (TOF smaller), and the mass resolution better.

Table 4. Summary of SWA-HIS performances at delivery.

	SWA-HIS requirement or needed inversion parameter	L1 or measured capability
Particle species	He ²⁺ , C ⁺⁴ to C ⁺⁶ ; O ⁺⁵ to O ⁺⁸ , Fe ⁺⁶ to Fe ⁺²⁰ , Mg ⁺⁶ to Mg ⁺¹² , Ne ⁺⁶ to Ne ⁺⁹ , Si ⁺⁶ to Si ⁺¹² , He ⁺ , C ⁺ , and O ⁺	H, ⁴ He, ³ He, C, N, O, Mg, Ne, Si, Fe (see Table 3 for details on masses and charges measured)
Energy per charge range	0.5–60 keV/e	0.5–~78 keV/e
Energy per charge resolution $\Delta E/E$ at FWHM	Between 6 and 10%	~8–9%
Mass resolution $M/\Delta M$ at FWHM	4	>5
Mass/charge resolution $(m/q)/\Delta(m/q)$	N/A	> 30
FoV		
In ecliptic	–33° to +66°	–33° to +66°
Out of ecliptic	±17°	±20°
Pixel resolution (Az × El)	6° × ~6° pixels	6° × ~4° pixels
G-factor/pixel (cm ² sr eV/eV)	N/A	~1 × 10 ^{–5}
Time resolution	≤30 s	4 s (Burst mode); 30 s (Normal mode); 300 s (Normal Low Cadence mode)

Notes. Rows colour-coded in blue show the Project-defined Level-1 requirements.

One of the science goals of SWA-HIS is the characterisation of the full VDF for pickup ions. As their typical charge state is +1, they gain only a single 25 keV step from the post-acceleration, as opposed to multiples of this value for higher charge states. For energies <10 keV, they do not produce a detectable energy signal in the solid state detector and therefore must be identified by their TOF only. Figure 15 shows a histogram of counts collected for a beam energy of 0.3 keV (25.3 keV after post-acceleration) representative of the characteristics of pick-up ions in the inner heliosphere; the beam was composed of 20% each of H₂, He, N₂, Ne, and Ar, with H₂O and CO₂ as contaminants in the chamber. Even at this very low energy, TOF measurement enables clear identification of the single-charge species.

3.3. The SWA Proton-Alpha System (SWA-PAS)

3.3.1. SWA-PAS introduction

SWA-PAS is designed to measure the 3D VDFs of solar wind protons and alpha particles with high time cadence, energy and angular resolution. In the solar wind, the proton and alpha-

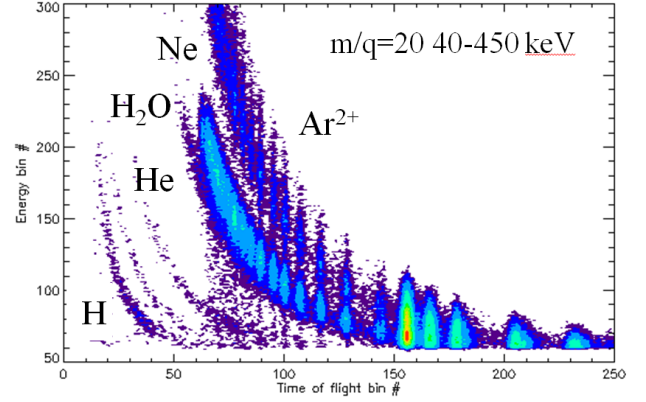


Fig. 14. E vs TOF spectrogram of $m/q = 20$ amu/e for various energy beams.

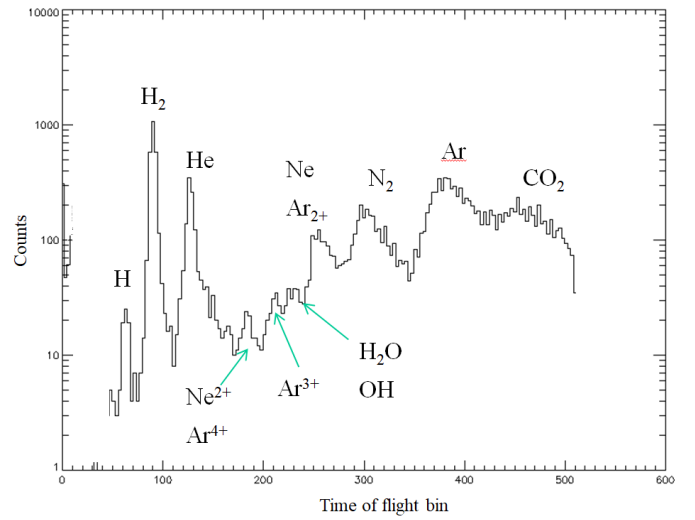


Fig. 15. Time-of-flight spectrum of a mixed beam of pickup ions of 0.3 keV energy.

particle thermal velocity is generally much smaller than the bulk velocity, which itself is usually strongly radially directed. Thus most of the individual ions within the distribution arrive at the spacecraft with at most a few 10²'s of degrees deviation from the radial direction. Thus SWA-PAS is mounted behind the spacecraft heat shield which has a dedicated cut-out in one corner. This cut-out allows a SWA-PAS FoV that covers the angular range of –22.5° to 22.5° in nine elevation (or polar) angle bins and has 11 azimuth angle bins covering a total width in this direction of 66°. In order to account for the expected aberration of the solar wind arrival direction due to the motion of the spacecraft, the FoV is offset from the solar direction by 9° such that the angular coverage is from –24° to +42°. In addition, the SWA-PAS sensor operates with a maximum resolution of 96 energy steps, from 200 eV/e to 20 keV/e.

The sensor will measure proton and alpha particle fluxes at a 4 s cadence, which will be returned to ground within the SWA telemetry stream. The SWA-DPU will also calculate moments of the associated distributions, which will be shared onboard with other instruments and returned to ground as a low-latency (<1 day following acquisition) data product for quick-look and mission planning purposes.

A complete 3D measurement of a VDF is a matrix of (96, 9, 11) elements (energy, elevation, azimuth), each element corresponds to the counts measured during a defined elementary time

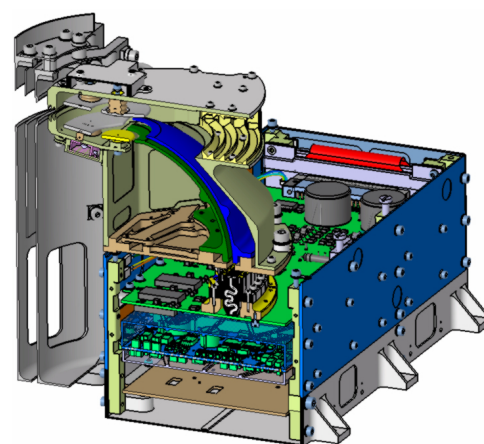
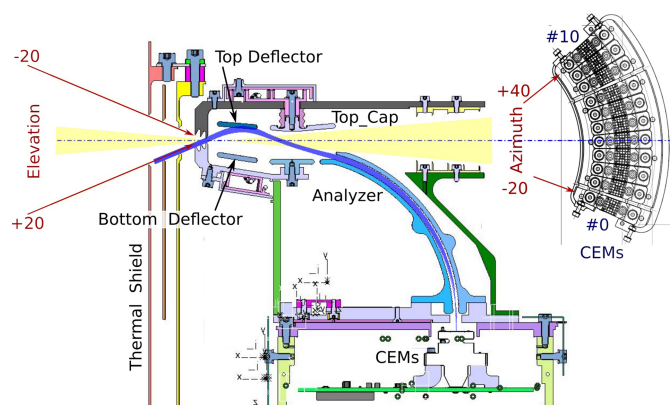


Fig. 16. *Left:* cut-away representation of the SWA-PAS analyser head. The cut-plane is that containing the Sun-spacecraft line and the direction of elevation deflection. The yellow shading represents the direct solar light and the blue curves show the extreme ion trajectories in this plane. The instrument has partial cylindrical symmetry extending from $+40^\circ$ to -20° out of the plane of the figure. *Right:* the insert shows the top view of the CEMs array detector arrangement and its angular range.

Fig. 17. Three-dimensional cut of the full SWA-PAS instrument illustrating the three main elements of SWA-PAS design: (1) the analyser (sensor head); (2) the electronics box containing the CEM detectors, HV sources, and other electronics boards; (3) the front thermal shield.

period by a specific bin. It is possible to reduce the number of energy and angular bins in one sample in order to significantly increase the sampling rate. SWA-PAS can automatically change the position of the reduced matrix to keep the maximum of the ion velocity distribution at the centre of the sampling window. Thus SWA-PAS is capable of taking a wide variety of “snapshot” and “burst” mode data products in which the time resolution of the sensor is increased. These high frequency modes consist of continuous acquisition of full or reduced VDFs, at second or sub-second cadences. The snapshot data products will be generated over periods of 8 s every 5 min in order to align with the operation of the RPW snapshot facility (Maksimovic et al. 2020; Walsh et al. 2020).

3.3.2. SWA-PAS design overview

Figure 16 shows the SWA-PAS sensor head which is comprised of the electrostatic analyser and an array of conventional channel electron multipliers (CEM) used to detect the solar wind ions. Since the instrument line-of-sight points to the Sun, the main driver of the sensor design was to provide reasonable defence against direct sunlight and heat radiation. In order to protect the sensor, it has a narrow aperture slit in front of the optical surfaces located outside of the solar light path through the sensor (yellow triangle in Fig. 16). This geometry avoids any interaction of the light beam with the internal elements of the sensor. The rear of the SWA-PAS analyser head is open to allow sunlight to pass straight through the head. In addition, the sensor has its own heat-shield system to locally protect the analyser.

The entrance deflection system, comprising two deflector plates and the “top-cap” plate, steers the incident particles towards the entrance of the electrostatic analyser. The deflection of the particles is achieved by applying specific potential on the plates. Figure 16 shows the ion trajectories calculated for the case of the maximum deflector voltages. The spherical shape electrostatic analyser filters out ions with energies outside a narrow energy band and focuses the remaining particles on to the CEM array. The azimuthal position of the focal point corresponds to the azimuthal direction of the incident ions. Thus the instant count rate of each CEM is a function of the solar wind ions flux in the corresponding bin of the SWA-PAS 3D sam-

pling matrix. The azimuth index of this bin is the CEM number, the energy index of the bin is defined by the electrostatic analyser instant voltage and the elevation index of the bin is defined by the deflector voltage to analyser voltage ratio. The averaged geometrical factor of one bin is $5 \times 10^{-6} \text{ cm}^2 \text{ sr eV eV}^{-1}$. This geometrical factor restricts the maximum count rate for an individual CEM to 10^7 s^{-1} when Solar Orbiter is at its closest approach to the Sun. Moreover, SWA-PAS still can produce a statistically valid 3D ion VDF every 4 s when the spacecraft is at 1 AU distance from the Sun. Details of the SWA-PAS measurement scheme are described in Sect. 3.3.3.

Figure 17 shows the three mechanical sections of SWA-PAS: the titanium multi-layer heat shield, the sensor head, and the electronics box. The sensor head is mounted on the top of the electronics box and is insulated from it thermally and electrically. The CEM detectors are located inside the box on the dedicated CEM board. The fast-varying HV voltages for the optical surfaces of the analyser head are generated by the HVPS. Other boards provide the HVPS controls, data acquisition, the SWA-DPU interface and LV power. We provide the details of these in Sect. 3.3.4.

Figure 18 shows the SWA-PAS assembly and its position on Solar Orbiter. The upper right insert shows the SWA-PAS installed on the spacecraft. SWA-PAS looks towards the Sun through a rectangular cut-out in a corner of the spacecraft heat-shield which has a stepped profile which acts to reduce the stray light. The charged particles pass across this cut-out, enter through the slot in the SWA-PAS heat shield, and then enter the sensor aperture. Most of the SWA-PAS external surfaces are protected by a high temperature “black Kapton” MLI. Other surfaces, shadowed against the solar heat flux, as well as against the heat radiation from other Solar Orbiter units, are coated by PCBE white paint and serve as radiators.

3.3.3. SWA-PAS measurement principle

A complete 3D measurement of an ion VDF is a matrix of (96, 9, 11) elements (energy, elevation, azimuth). Each bin of this matrix corresponds to the counts measured during a defined elementary time period of $\sim 1 \text{ ms}$ by a specific channeltron, for a given energy and elevation angle bin. SWA-PAS accumulates counts in all azimuthal bins simultaneously, but to cover all